Gaussian algorithm for retrieving and projecting aerosols optical depth: A case study of Monrovia-Liberia

M Emetere*1,2

- 1. Department of Physics, Covenant University Canaan land, Nigeria.
 - 2. Department of Mechanical Engineering Science, University of Johannesburg, South Africa

ABSTRACT

The large loss of satellite datasets over most parts of West Africa is very dangerous for the purpose of nowcast and forecast. The cause was traced to salient inabilities for satellite sensors to separate aerosols radiances from the surface of the earth to the top of the atmosphere. Fourteen years (2000-2013) Multi-angle Imaging Spectro Radiometer (MISR) was obtained. The volume of data loss in fourteen years was given as 69.9%. Guassian algorithm technique (GAT) was used in this study to retrieve the missing data for fourteen years. The success of the operation extended the research exploration to forecasting twenty years aerosols optical depth. GAT was proven to be very consistent via statistical analysis, cotour mapping, surface mesh mapping, relief mapping and vector mapping. A very high aerosol loading is expected to commence at the begining of 2023 and may last till 2028. It was also shown that aerosol optical depth may be stable between 2029-2033. Two hypothesis were propounded for further work. The results show that aerosol loading over the region is high and may be a major source of environmental hazard in the nearest future.

1. INTRODUCTION

Data loss in most satellite database over some parts of West Africa is worrisome. This anomaly would definitely affect the comprehension of the health implication of polluted atmosphere, as well as the climate nowcast and forecast. Based on the above, several studies have been dedicated to modeling of aerosols optical depth (AOD), aerosols loading and aerosols retention with moderate degree of accuracy. For example, the multilayer analysis of a ground-based sun photometer of aerosol optical properties was carried out by Oluleye et al. (2012). Its outcome was compared with satellite observations over West Africa. Daily observations of satellite imaging of aerosol precipitations were made from 2005 – 2009 at three sites in West Africa and in an area within the Atlantic Ocean. Specific locations observed include Agoufou area of Mali, Banzoumbou area of Niger, Cape Verde in Tropical Atlantic Ocean and Ilorin Area of Nigeria. The results of the findings showed that the AOD for the four stations had different influence on the annual precipitation, temperature and relative humidity. Spatial, seasonal and interannual variation of the aerosol loading over sahelian West Africa were detected by satellite (MODIS and TOMS) and ground-based AERONET Sunphotometer

^{*}Corresponding Author: emetere@yahoo.com

sensor between 2005-2009. The result showed that the Moderate resolution imaging spectro radiometer (MODIS) and TOMS retrieved as a ratio of aerosol optical depth to the aerosol interval AOD/AI were in good agreement with ground-based AERONET data.

Yang et al (2014) carried out a study on the simulation of aerosol dynamics which includes a comparative review of algorithms used in Air Quality Models. The paper was focused on four areas including coagulation, condensational growth, nucleation, and gas particle mass transfer. It was shown that sectional approach has the capacity to make good predictions for coagulation and condensational growth phenomena. The numerical solution adopted to describe the condensational growth rate of particles in the range of 0.001-10 µm has its limitation in the area of 3D simulation. This limitation is tied to the algorithm of the operating satellite system. Over the years, there have been attempt to propound a more accurate retrieving algorithm to improve upon the AOD output. The MAIAC algorithm is a popular aerosol retrieval technique for atmospheric correction scheme over land for MODIS data (Lyapustin et al., 2011). There are other algorithms used for aerosols retrieval purposes (Knapp et al., 2005; Levy et al., 2007; de Almeida et al., 2007; Bilal et al., 2014). Zhang et al. (2011) rightly identified the challenges of retrieving satellite aerosol optical depth which is hinged on the inability to separate the contributions of aerosols radiances from the surface to the top of the atmosphere. Till date, the problem still persists despite the numerous studies done.

The West Africa Regional Scale Dispersion Model (WARSDM) was propounded to address the peculiar climate influence on aerosols dispersion over West Africa (Emetere et al., 2015a, b, c; Emetere 2016, Emetere et al., 2016a, b). Different atmospheric constants for different locations across West Africa were considered to help the configuration settings of aerosol measuring instruments to optimally function. The execution of the model in over fifty towns in West Africa has shown high success. The limitation of WARSDM is the dynamism of the atmospheric constants as it relates to the significant influence of climate change. Hence, the dataset obtained from WARSDM may be deviating from the estimated values if the instantaneous atmospheric constant is not known. The shortcoming of WARSDAM propelled this study to seek for a complimentary tool that would generate significant verification table to ascertain the accuracy of the estimated dataset.

2. METHODOLOGY

Only very few aerosols ground observation is available in West Africa. Hence, the satellite observation was adopted. Fourteen years (2000-2013) satellite observation was obtained from the Multi-angle Imaging SpectroRadiometer (MISR). The MISR operates at various directions i.e. nine different angles (70.50, 600, 45.60, 26.10, 00, 26.10, 45.60, 600, 20.50) and gathers data in four different spectral bands (blue, green, red, and near-infrared) of the solar spectrum. The blue band is at wavelength 443nm, the green band is at wavelength 555nm, the red band wavelength 670nm and the infrared band is at wavelength 865nm. MISR acquire images at two different levels of spatial resolution i.e. local and global mode. It gathers data at the local mode at 275 meter pixel size and 1.1 km at the global mode. Typically, the blue band is to analyze coastal and aerosol studies. The green band is to analyze Bathymetric mapping and estimating peak vegetation. The red band analyzes the variable vegetation slopes which includes the infrared band analysis of biomass content and shorelines.

The raw MISR dataset was processed using the Excel package. The mean for each month were calculated for each year. The accuracy of the data was tested by applying the aerosol dispersion model that was propounded by Emetere et al. (2015a, b) which is shown in equation (1):

$$\psi(\lambda) = a_1^2 \cos\left(\frac{n_1 \pi \tau(\lambda)}{k_v} + \alpha\right) \cos\left(\frac{n_1 \pi \tau(\lambda)}{k_z} + \alpha\right) + a_2^2 \cos\left(\frac{n_2 \pi \tau(\lambda)}{k_v} + \beta\right) \cos\left(\frac{n_2 \pi \tau(\lambda)}{k_z} + \beta\right)$$
(1)

Here α and β are the phase differences, k is the diffusivity, τ is the AOD, ψ is the concentration of contaminant, λ is the wavelength, a and n are atmospheric and tuning constants respectively.

The second technique involves the application of the different Gaussian equation to derive the missing data in the year. Different statistical tools or parameters were used to guide the results. For example, the sum of squared errors (SSE) of prediction is used to monitor the unrealistic estimated data; the R2 value was used to measure how close the data are to the fitted regression line; the Root Mean Square Error (RMSE) shows how close the observed data points are to the model's predicted values; the adjusted R-squared was used to validate or test the predictors of the regression system.

After filling the empty spaces in the years between 2000 and 2013, the results were used to predict the AOD data for twenty years using equation (2). After the fifteen years prediction, AOD constant of 0.5 was added to equation (2) to sustain the AOD trend i.e. equation (3).

$$f(x) = a_1 \exp\left(-\left(\frac{(x - b_1)}{c_1}\right)^2\right) + a_2 \exp\left(-\left(\frac{(x - b_2)}{c_2}\right)^2\right) + a_3 \exp\left(-\left(\frac{(x - b_3)}{c_3}\right)^2\right) + a_4 \exp\left(-\left(\frac{(x - b_4)}{c_4}\right)^2\right)$$
(2)

$$f(x) = a_1 \exp\left(-\left(\frac{(x - b_1)}{c_1}\right)^2\right) + a_2 \exp\left(-\left(\frac{(x - b_2)}{c_2}\right)^2\right) + a_3 \exp\left(-\left(\frac{(x - b_3)}{c_3}\right)^2\right) + a_4 \exp\left(-\left(\frac{(x - b_4)}{c_4}\right)^2\right) + 0.5$$
(3)

3. RESULTS AND DISCUSSION

Monrovia has the highest cases of scanty data in the locations considered (Figure 1). There were little or no data from March to November (Figure 1). Since Monrovia falls within the tropical monsoonal climate, the scanty AOD data may be as a result of the moisture content (Adebiyi et al., 2015), cloud scavenging (Dani et al., 2003), precipitable water content (Vijayakumar and Devara, 2013) and high rain drop rate (Boucher and Quaas, 2013). Hence, attempts to unravel the contributions of aerosols radiances from the surface to the top of the atmosphere in such region may be a goose chase at the moment (Zhang et al., 2011). The Tropical Rainfall Measuring Mission (TRMM) layer 3 observations in Figure 2 show the daily rain rate in Monrovia for the year 2012 while Figure 3 shows a monthly rain rate analysis. Hence, it can be affirmed that the scanty AOD data was as a result of the rain rate that is higher within May and October as shown in Figure 1.

The AOD pattern over Monrovia agreed with the WARSDAM model (Figure 4). Monrovia is constantly under the oceanic wind influence from the Atlantic oceanic. The retrieved AOD may not capture salient events in the lower atmosphere without the installation of radiosonde station to adequately capture the inadequacies in its lower atmosphere.

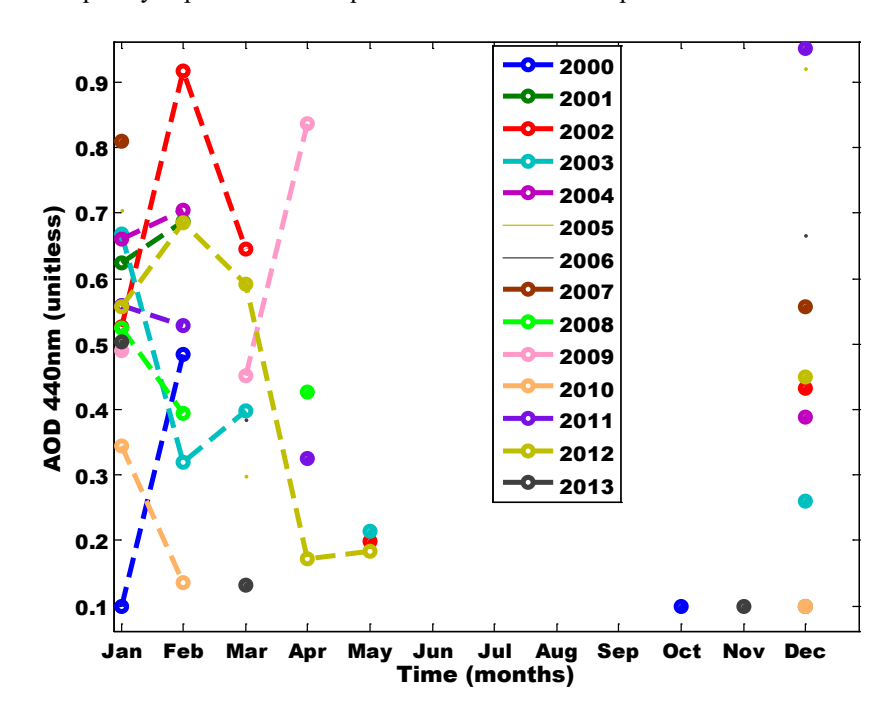


Figure 1: AOD pattern for Monrovia (2000 - 2013)

The main aim of this paper is to seek for a complementary technique to the WARSDM. The potential of the Gaussian algorithm technique (GAT) was explained by considering the raw data, estimated data within same time-frame and the predictive data. The statistical analysis of the raw dataset is shown in Table 1 & 2 below

Table 1: Statistical analysis of the raw dataset (2000-2006)

Parameters	2000	2001	2002	2003	2004	2005	2006
Number of values	3	3	5	5	3	3	3
Minimum	0.1	0.1	0.199	0.215	0.388	0.298	0.384
Maximum	0.484	0.688	0.9175	0.668333	0.7045	0.921	0.666
Mean	0.228	0.47075	0.5443	0.372567	0.58443	0.641	0.5177
Standard error	0.128	0.186286	0.11865	0.080059	0.099024	0.1826	0.08174
Standard deviation	0.2217	0.322657	0.26532	0.179017	0.17151	0.3162	0.1416
Coefficient of							
variation	0.97238	0.68541	0.48745	0.4805	0.29347	0.49336	0.27348

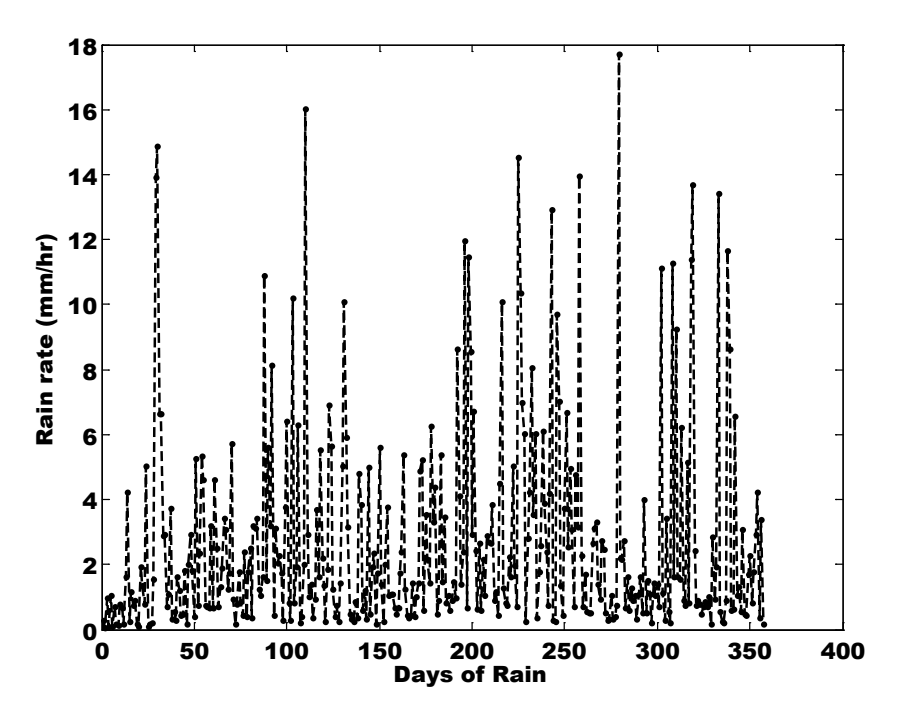


Figure 2: Daily Precipitation rate over Monrovia 2012

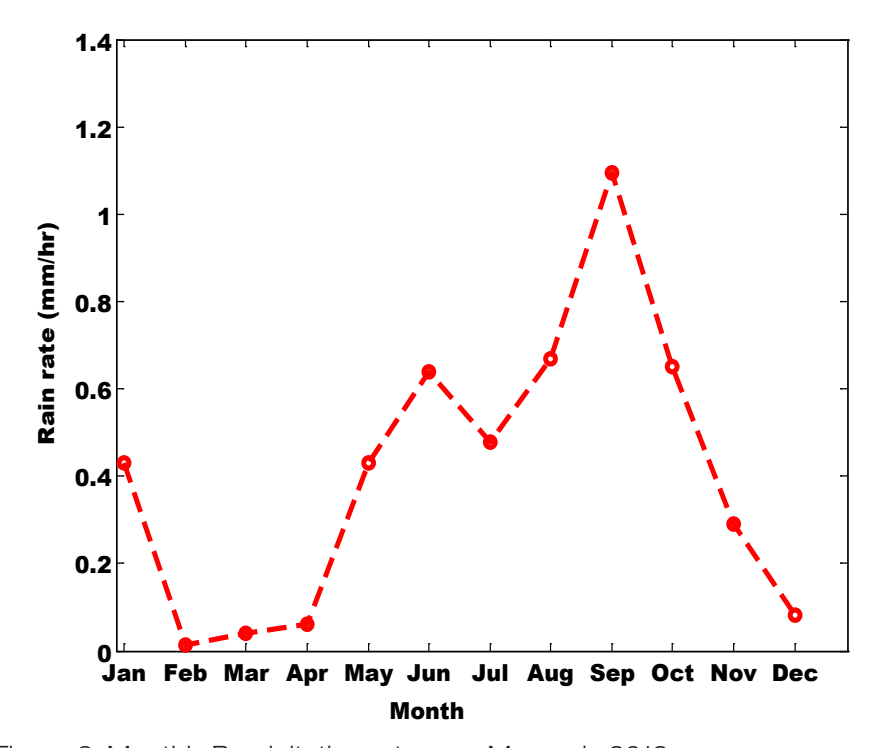


Figure 3: Monthly Precipitation rate over Monrovia 2012

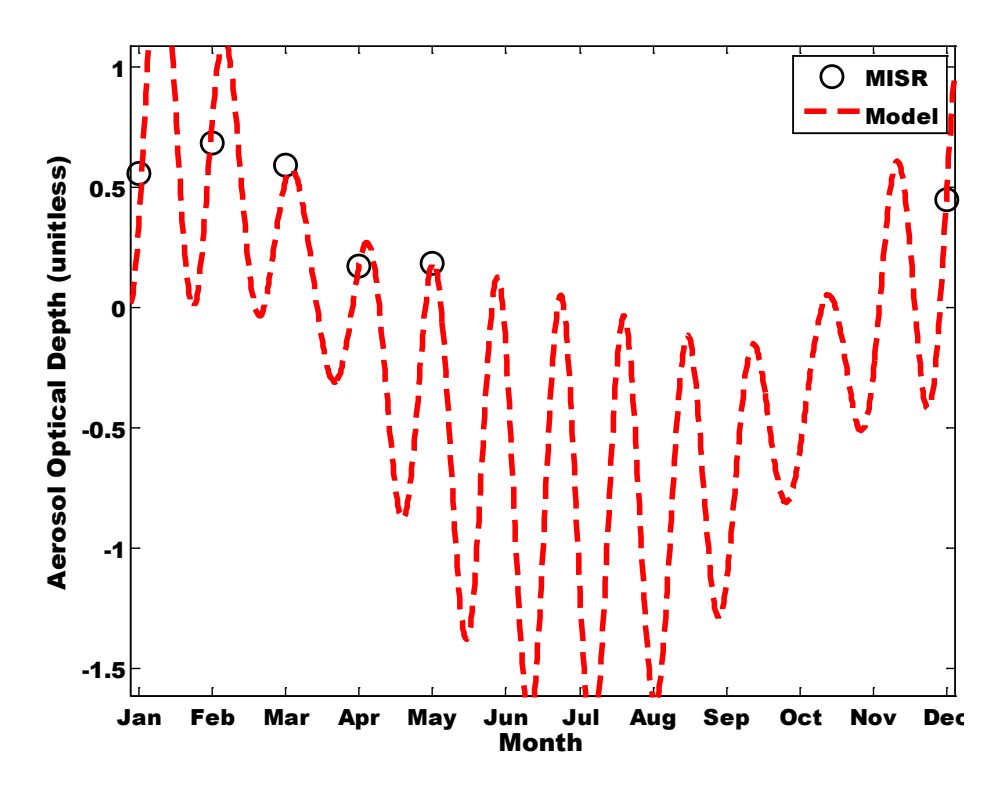


Figure 4: AOD for new model and MISR for the year 2001

Table 2: Statistical analysis of the raw dataset (2007-2013)

Parameters	2007	2008	2009	2010	2011	2012	2013
Number of values	2	4	4	3	4	6	3
Minimum	0.5575	0.1	0.1	0.1	0.326	0.1715	0.1
Maximum	0.81	0.5235	0.836	0.345	0.952	0.685333	0.504
Mean	0.68375	0.36088	0.469167	0.1933	0.591062	0.439611	0.2453
Standard error	0.12625	0.091215	0.15043	0.0765	0.1309	0.088477	0.1297
Standard deviation	0.17854	0.18243	0.30086	0.1325	0.2618	0.216724	0.2246
Coefficient of							
variation	0.26113	0.50552	0.64126	0.68539	0.44293	0.49299	0.91542

The year 2007 had the least AOD data i.e. 2. Most of the month had only three data. The year 2012 had the highest volume of data i.e. 6. Hence, the volume of data lost can be calculated as:

$$Data\ loss = \left(1 - \frac{number\ of\ outcomes}{Expected\ outcomes}\right) \times 100\%$$

Hence, there is 69.6% data loss within fourteen years in Monrovia. This is a major problem in major town and cities in West Africa (Emetere, 2016). However, there are still some information that can be inferred from Tables 1 & 2. For example, the AOD over Monrovia can be as high as 0.952 as shown in the year 2010. This means that the research site requires 'ground-truthing' to ascertain the level of danger on the life-forms. The polynomial and Gaussian curve-fitting technique were used to fill-in the lost dataset (as shown in Tables 3 & 4).

Table 3: Statistical analysis of the treated dataset (2000-2006)

Parameters	2000	2001	2002	2003	2004	2005	2006
Number of values	12	12	12	12	12	12	12
Minimum	-0.956	0.10008	-0.96369	0.234475	0.388	0.0602	0.329408
Maximum	1.06	0.74864	0.79072	0.630751	0.7534	0.9212	0.666092
Mean	0.452	0.566388	-0.04949	0.342012	0.64998	0.358825	0.433163
Standard error	0.182428	0.060947	0.192186	0.031588	0.033775	0.08134	0.030456
Standard deviation Coefficient of	0.631949	0.211126	0.665753	0.109423	0.117	0.281771	0.105504
variation	1.39812	0.37276	-13.4532	0.31994	0.18	0.78526	0.24357

Table 4: Statistical analysis of the treated dataset (2007-2013)

Parameters	2007	2008	2009	2010	2011	2012	2013
Number of values	12	12	12	12	12	12	12
Minimum	0.2464	0.0999	0.1036	-0.3519	-0.0059	0.1726	-0.1752
Maximum	0.8105	0.8267	2.7033	0.345	0.9515	3.0232	0.504
Mean	0.42366	0.55128	1.42184	-0.08948	0.3244	1.18651	0.048233
Standard error	0.051117	0.062381	0.28044	0.068703	0.082515	0.298003	0.062315
Standard deviation Coefficient of	0.17707	0.21609	0.971472	0.23799	0.28584	1.03231	0.21586
variation	0.41796	0.39198	0.68325	-2.65963	0.88114	0.87004	4.47542

It was observed that the adopted process gave a detailed summary of the AOD over Monrovia. First, it was observed that the AOD can be as high as 3.0232. Also, the maximum AOD throughout the years had been high. This shows that the research site is currently having excess deposition of air pollution into the atmosphere. These results affirmed UN report that an estimated 6.5 million deaths (11.6 per cent of all global deaths) were associated with indoor and outdoor air pollution (UN, 2016). The validity of the process can be seen from the standard error which was quite low. Also, the standard deviation shows that the dataset is within accuracy. The negative value of the coefficient of variation for the year 2002 and 2010 may be misleading i.e. judging from the trivial interpretation. The negative coefficient cannot be related to the magnitude of the AOD because the minimum AOD recorded at 2002 and 2010 are given as -0.96369 and -0.3159. It should be noted that negative AOD is possible as put forward by Moderate Resolution Imaging Spectroradiometer (MODIS). This is to avoid an arbitrary negative bias at the low AOD end in long term statistics (MODIS, 2017). Also, it was reported that MODIS does not have sensitivity over land to retrieve aerosol to better than +/-0.05. In statistical practice, when all the dataset in a long-term statistic is kept positive, an

Table 5: Gaussian coefficients and statistical justification

Dec	Nov	Oct	Sep	Aug	Jul	Jun	May	Apr	Mar	Feb	Jan	Month
1.085	3.994	6,078	3.094	793.4	28.12	2.611	9.446	1.622	4.414e+013	0.7861	0.8056	a_1
12.33	13.42	9.611	9.782	9.522	9.542	9.778	9.549	-7.481	-20.43	2.489	12.47	b_1
0.8032	0.7933	0.4322	0.6849	0.1981	0.2791	0.6639	0.3234	11.95	3.78	2.014	0.4354	c_1
0.9305	2.317	2.698	827.4	1.721	2.489	1.633	1.079	224.5	0.3966	0.7624	65.92	a_2
6.888	9.812	12.91	13.56	13.47	1.453	13.47	1.18	9.524	4.979	12.79	12.12	b ₂
2.64	0.5921	0.4635	1.676	0.6596	0.4907	0.6915	1.348	0.1968	0.4027	1.237	4.936	c_2
-73.24	-4.2c+013	5.695	-825	24.83	0.8023	11.5	1.581	1.91	0.6532	2.488	0.4616	a_3
8.457	24.47	14.84	13.56	1.487	13.94	1.478	15.14	4.634	2.511	5.454	3.018	<i>b</i> ₃
0.6282	1.84	0.8206	1.679	0.2701	1.215	0.301	1.51	0.3611	0.7676	0.3538	2.089	C ₃
87.05	0.4978	0.6406	1.303	0.6953	0.7961	0.4029	0.7735	-0.5216	0.3567	0.5913	-65.61	a_4
8.465	7.382	5.133	-0.6244	4.92	4.805	5.473	4.871	4,469	8.078	8.046	12.11	b ₄
0.5537	3.183	1.117	2.256	0.9469	0.7473	2.972	0.7788	1.77	13.56	2.005	4.876	c_4
1.142	1.106	1.793	1.775	0.669	0.34	0.2162	0.3193	0.193	0.2599	0.02208	0.1099	SSE
-1.628	0.4646	0.1818	0.01253	0.3567	0.4739	0.7194	0.1725	0.08025	-1.243	0.6967	-0.9389	Adjusted R ²
0.5957	0.9176	0.8741	0.8481	0.901	0.9191	0.9568	0.8727	0.8585	0.655	0.9533	0.7017	2 R2
0.7555	0.7436	0.9468	0.942	0.5784	0.4123	0.3288	0.3996	0.3106	0.3605	0.1051	0.2344	RMSE

artificial bias emerges. (NOAA) further affirmed that negative tendency is more evident in globally and annually averaged AOD (NOAA, 2017). Therefore, the negative coefficient of variation is not misleading via the aforementioned realities. Hence, the high coefficient of variation at 2000 and 2013 may not be misleading because it means that both years had a low degree of returns.

The mean and standard deviation in 2009 and 2012 were very high compared to other years. This means that the missing data were very high compared to the values given in Table 2. This leads to the first hypothesis that missing dataset over West Africa is very high; hence, the satellite sensor cannot comprehend it. This hypothesis can be supported by satellite imageries over West Africa. The success of the statistical analysis prompted the further consideration of the analysis of twenty years forecast. Equation (2) was used for the first fifteen years while equation (3) was used for the last five years. The coefficient of the Gaussian algorithm technique is shown in Table 5 below. The analysis was considered for a monthly event. This would ensure that the analysis of the corresponding years would be independent, bias-free and accurate. a_1 coefficient is very high in the month of March for 20 years. Coincidentally, the adjusted R-square was the lowest. The month of April had the highest c_1 and a_2 coefficients. Summarily, the months between August and April had the highest coefficients. This result tallies with the trend of aerosol optical depth in West Africa (Emetere et al., 2016a). The high trend of R-squared was between May and August. Here, it could be inferred from the rain rate diagrams in Figures 2 & 3 that it still has a significant role in the nearest future in the research area. Hence, the GAT has shown high degree of accuracy even for forecast purposes. It is salient to note that the error analysis gave more credence to the accuracy of the Gaussian algorithm technique.

The statistical analysis of the forecast dataset is shown Tables 6-8.

Table 6: Guassian prediction of the treated dataset (2014-2020)

Table 6: Guass	sian predic	SHOTI OF LITE	e treated da	alasel (20	114-2020)		
Parameters	2014	2015	2016	2017	2018	2019	2020
Number of							
values	12	12	12	12	12	12	12
Minimum	0	0.0002	0.0024	0.0195	0.0026	0.0002	0
Maximum	1.0615	0.7898	0.7462	0.6467	0.7529	0.8309	0.6704
Mean	0.605258	0.49388	0.2745	0.28776	0.56982	0.32888	0.27033
Standard error	0.1263	0.090656	0.084155	0.044321	0.067173	0.0684670	0.073449
Standard							
deviation	0.437516	0.31404	0.29152	0.15353	0.23269	0.23718	0.25443
Coefficient of							
variation	0.72286	0.63586	1.062	0.53355	0.40836	0.72116	0.94119

It was noticed that the fifteenth to the eighteenth year had a missing data each. This led to the second hypothesis that long term AOD statistics would naturally generate zero AOD value. As opposed to the operation analysis of MOD04_L2, the GAT was not influenced or manually adjusted in the first fifteen years. The sixteenth to the eigteenth year were adjusted by the introduction or addition of 0.5 as shown in equation (3). Unlike Table 3 & 4, there were no negative coefficient of variation. This may mean that the Gaussian algorithm technique may

be extended above 20 years. We calculated to 30 years but discovered that the AOD outcome converged to zero for dataset between June and August. Hence, the GAT may be valid for 20 years only. Lastly the validity of the GAT was tested using the cotour mapping, surface mesh mapping, relief mapping and vector mapping.

The contour map of the forecast shows three features i.e. evenly spaced, widely spaced and jagged contours (Figure 5) which indicates uniform slope region A, gentle slope region B and tropospheric pertubations region C respectively. This analysis confirm that the predicted dataset is largely reliable.

Table 7: Gaussian prediction of the treated dataset (2021-2027)

Parameters	2021	2022	2023	2024	2025	2026	2027
Number of values	12	12	12	12	12	12	12
Minimum	0	0.0182	0.0965	-0.3056	-0.0655	0.086	0.015
Maximum	0.6366	0.8281	2.7036	0.3405	0.9384	3.0392	2.0506
Mean	0.26354	0.57435	1.46927	0.091258	0.23218	1.04268	0.897792
Standard error Standard	0.076287	0.068704	0.298146	0.049402	0.086807	0.278388	0.214351
deviation	0.26426	0.238	1.03281	0.17113	0.30071	0.964364	0.742533
Coefficient of variation	1.00274	0.41438	0.70294	1.87528	1.29514	0.92489	0.82707

Table 8: Gaussian prediction of the treated dataset (2028-2033)

Parameters	2028	2029	2030	2031	2032	2033
Number of values	11	11	11	11	12	12
Minimum	0.5001	0.0356	0.3504	0.4834	-0.0006	-0.0115
Maximum	5.9826	1.643	1.3058	1.1988	1.0378	0.8698
Mean	1.30877	0.759636	0.6361	0.605518	0.535292	0.51633
Standard error	0.487592	0.140692	0.079536	0.064352	0.067112	0.058355
Standard deviation Coefficient of	1.61716	0.466623	0.263792	0.21343	0.232481	0.20215
variation	1.23563	0.61427	0.4147	0.35247	0.43431	0.39151

The thick coloured line in the surface mesh mapping (Figure 6) showed the implication of line 0.1 in Figure 5. This means that the turbulence was initiated by the 0.1 line. Also, beyond the 0.1 line i.e. 0.35 line it showed that a normalized state may lead to a steady linear state. Hence, Figure 6 show that the Guassian algorithm technique would perfectly mimic or trend the event in the source dataset and evenly show its signatures in an extensive forecast purpose.

The relief mapping of the forecast dataset (Figure 7) show that the possibility of two very high data (red circle) and two low data (blue circle). This further show that the dataset is very stable and maybe regarded as accurate. The vector mapping basically showed the low resolution (level 0), medium resolution (level 1) and high resolution (level 2) further confirm both the horizontal and vertical accuracy of the predicted dataset (Figure 8).

Since the Gaussian algorithm technique has been shown to be accurate, it can be relied upon to discuss future events in the research area. Lastly, the cumulative 3D plot of the twenty

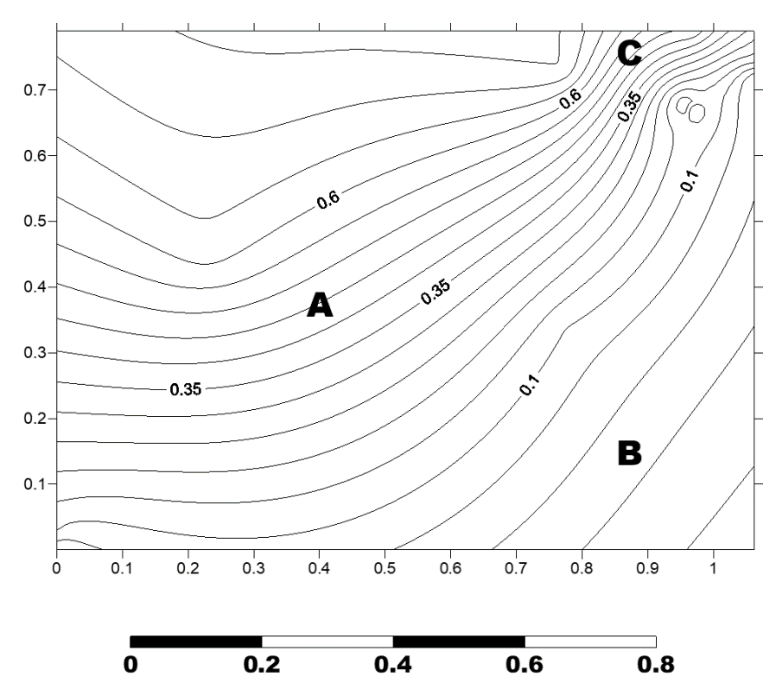


Figure 5: Contour mapping of forecast dataset.

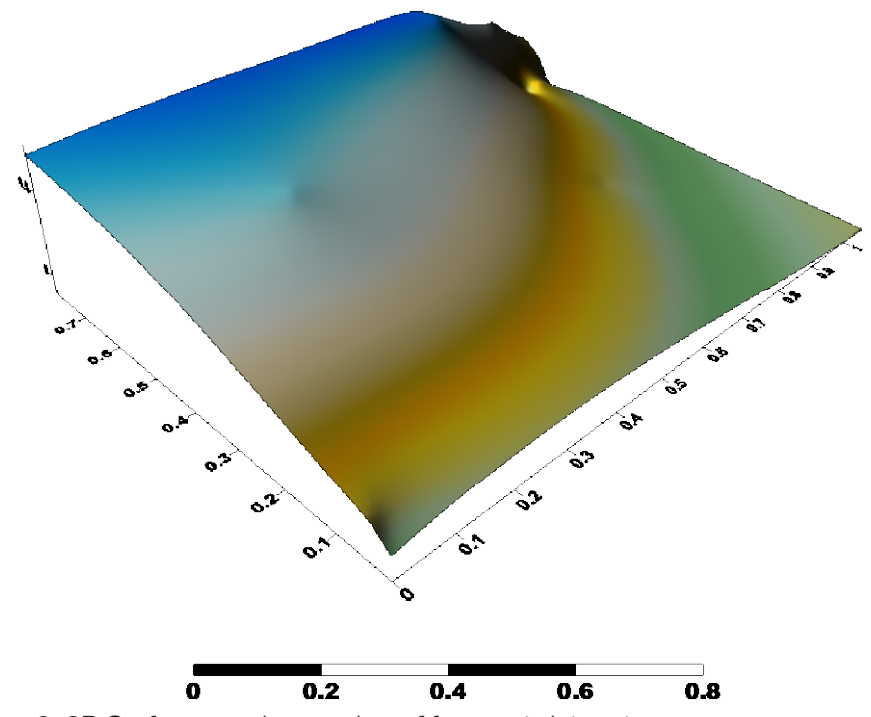


Figure 6: 3D Surface mesh mapping of forecast dataset.

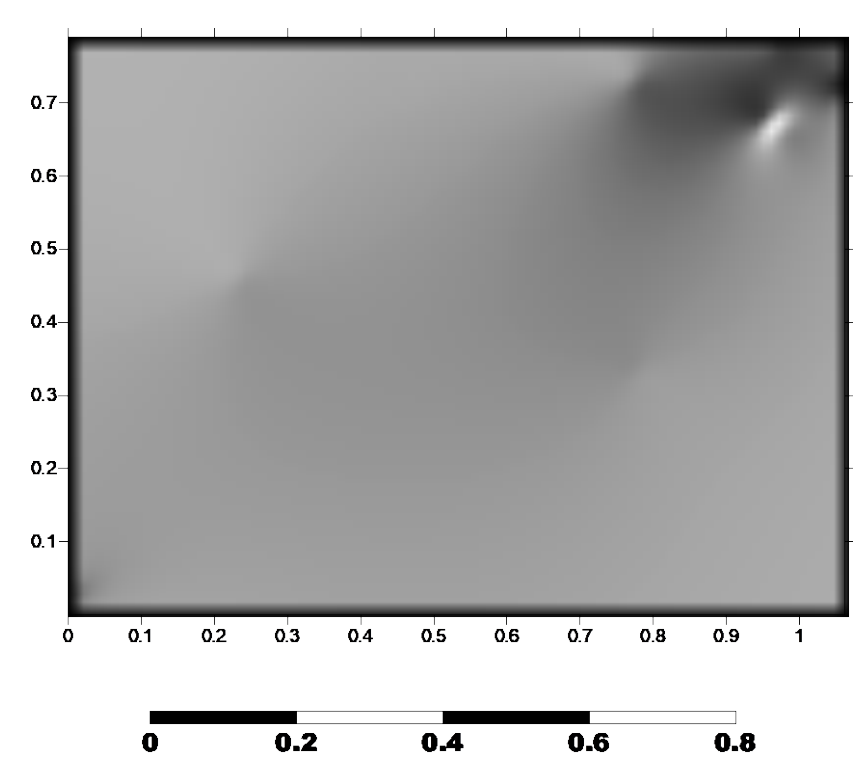


Figure 7: 3D Relief mapping of forecast dataset.

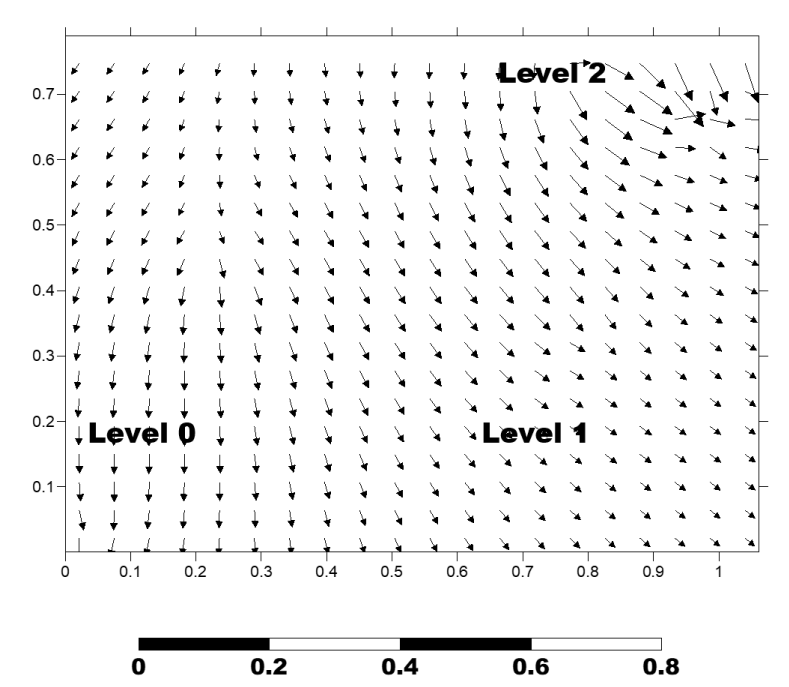


Figure 8: Vector mapping of forecast dataset.

years was done in Figure 9 to further interpret the graph. Turbulent aerosol loading is expected between 2025 to 2030. Hence, the twenty years was divided into two halves i.e. 10 years apart and plotted as shown in Figures 10 & 11.

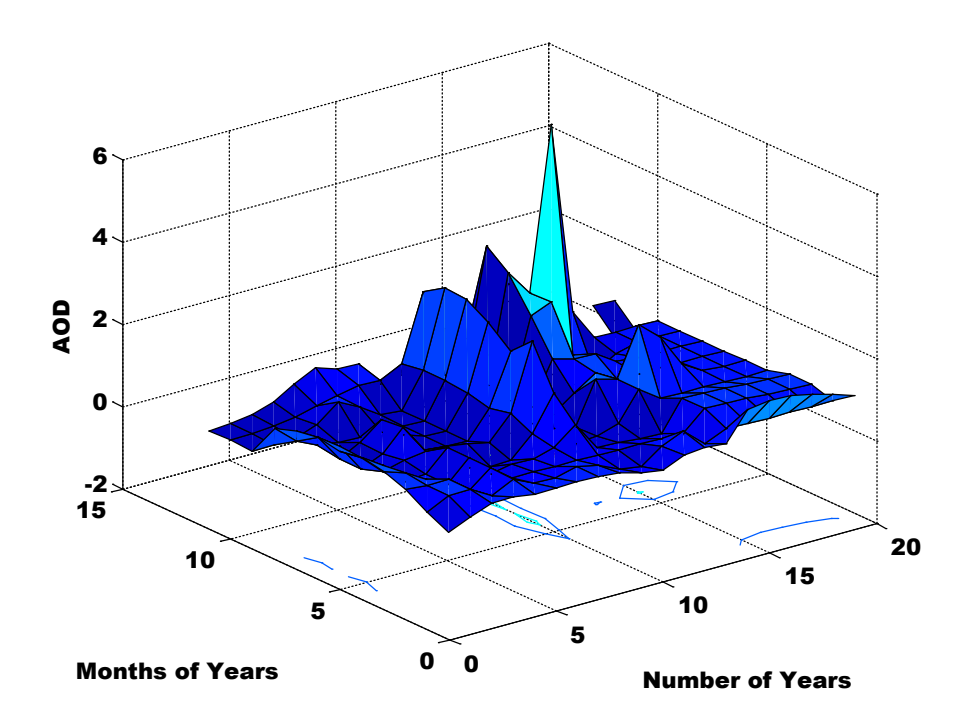


Figure 9: 3D plot for twenty years forecast data

Figure 10 show that the AOD for late 2017 to 2020 may be slightly high. A very high aerosol loading is expected to commence at the begining of 2023. This is due to large aerosols retention in the atmosphere (Emetere, 2016) and the long life time of the aerosols (Poschl, 2005). Figure 11 show that aerosol optical depth may be stable between 2029-2033 because of the complete decay of retained aerosols in the atmosphere. This assumption is only possible if there is a minimal anthropogenic pollution over the research site i.e. Monrovia. The bar chart of the monthly performance for twelve years in Figure 12 further corroborated the findings in Figures 9-11. Hence, the Gaussian algorithm technique is very consistent in nowcast, forecast and interpretation of events.

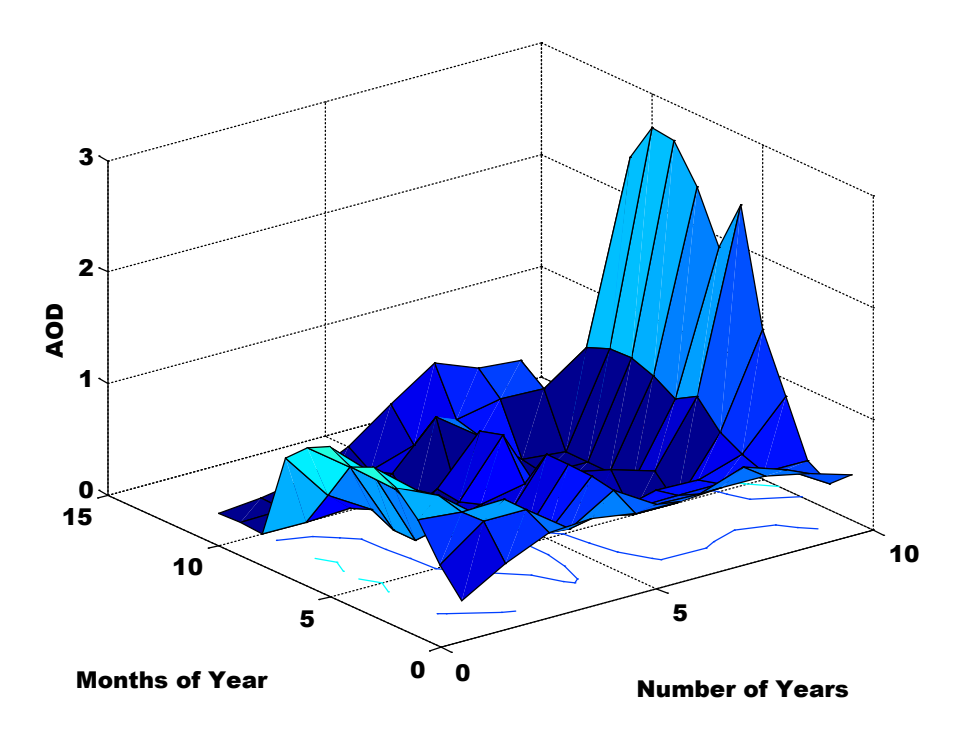


Figure 10: 3D plot for the first ten years forecast data

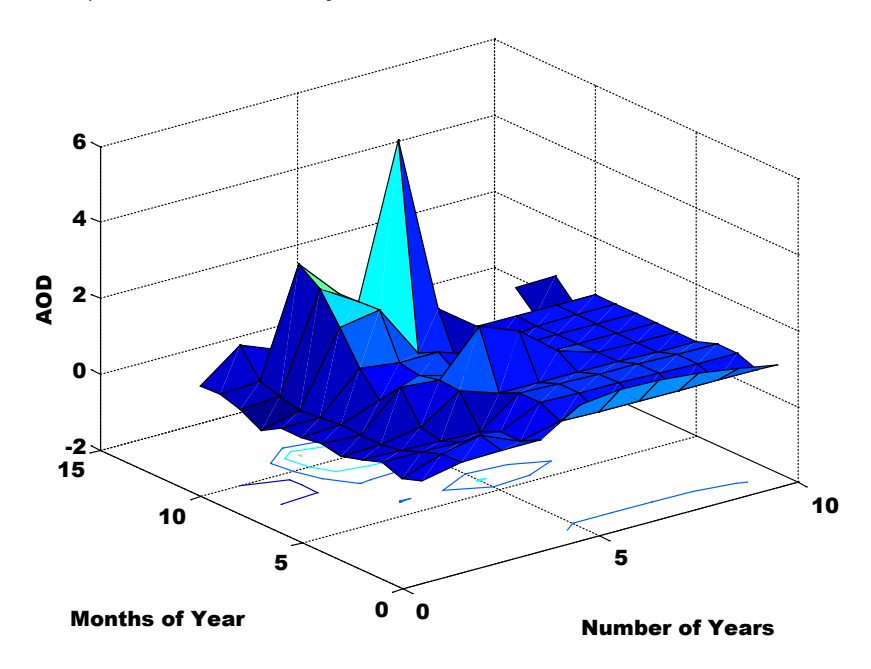


Figure 11: 3D plot for the last ten years forecast data

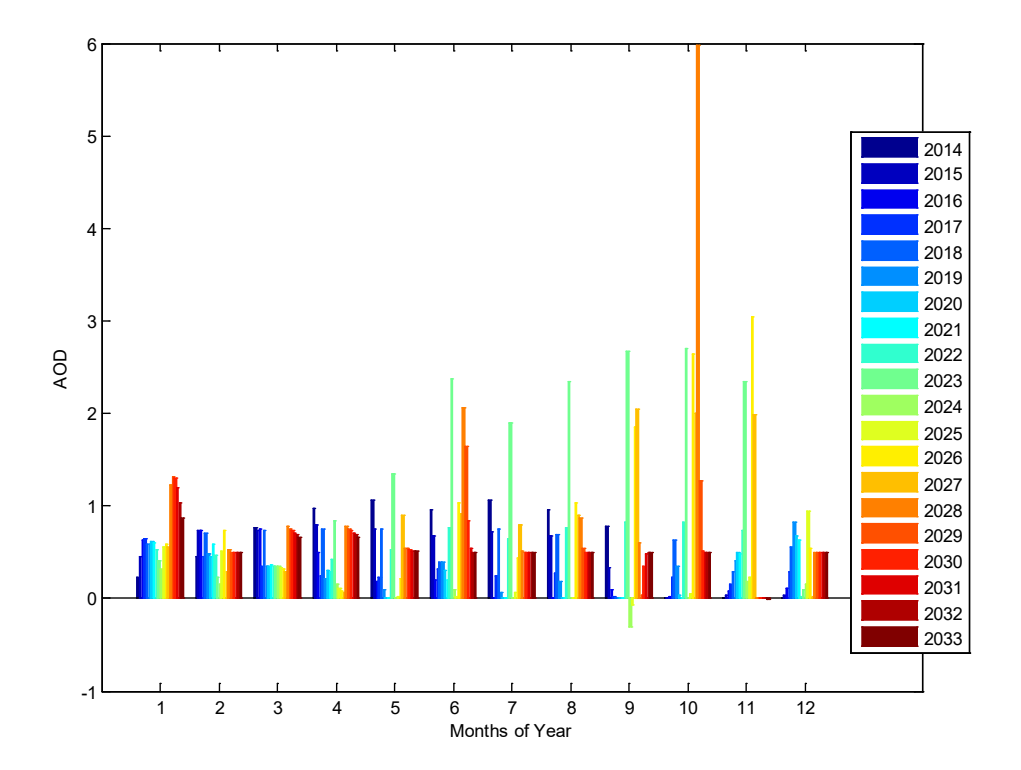


Figure 12: Bar chart of the monthly performance for twelve years

4. CONCLUSION

The aerosols loading over Monrovia is very high. The aerosol loading over the study site is largely influenced by rain rate and aerosols decay. The Gaussian algorithm technique have been proven to be very consistent via statistical analysis, cotour mapping, surface mesh mapping, relief mapping and vector mapping. Hence, the GAT is recommended for nowcast, forecast and interpretation of events. A very high aerosol loading is expected to commence at the begining of 2023 and may last till 2028. It was also shown that aerosol optical depth may be stable between 2029-2033. Two hypothesis were propounded for further work. In general, environmental authorities in Liberia are advised to ameliorate the continuous aerosols loading over the region to prevent cases of partial famine in the nearest future.

ACKNOWLEDGEMENT

The author acknowledges the assistance from NASA to use their satellite dataset.

REFERENCES

- [1] Adebiyi, A.A., Paquita, Z. and Steven, J.A., (2015): The convolution of dynamics and moisture with the presence of shortwave absorbing aerosols over the southeast atlantic. Journal of Climate, 28: 1997–2024.
- [2] Bilal, M., Nichol, J. E., and Chan, P. W. (2014): Validation and accuracy assessment of a Simplified Aerosol Retrieval Algorithm (SARA) over Beijing under low and high aerosol loadings and dust storms, Remote Sens. Environ., 153, 50–60

- [3] Boucher, O. and Quaas, J., (2013): Water vapour affects both rain and aerosol optical depth, Nature Geosciences, 6: 4–5
- [4] Dani, K.K., Maheskumar, R.S., and Devara, P.C.S., (2003): Study of total column atmospheric aerosol optical depth, ozone and precipitable water content over Bay of Bengal during BOBMEX-99. Journal of Earth System Science, 112 (2): 205-221.
- [5] de Almeida Castanho, A. D., Prinn, R., Martins, V., Herold, M., Ichoku, C., and Molina, L. T. (2007): Analysis of Visible/SWIR surface reflectance ratios for aerosol retrievals from satellite in Mexico City urban area, Atmos. Chem. Phys., 7, 5467–5477
- [6] Emetere Moses E., Akinyemi M.L. & Oladimeji T.E. (2016a): Statistical Examination Of The Aerosols Loading Over Kano-Nigeria: The Satellite Observation Analysis, Scientific Review Engineering and Environmental Sciences, 72: 167-176
- [7] Emetere, Moses Eterigho, (2016): Statistical Examination of The Aerosols Loading Over Mubi-Nigeria: The Satellite Observation Analysis, Geographica Panonica, 20(1), 42-50
- [8] Emetere Moses E., Akinyemi M.L. & Akinwumi S.A. (2016b): Aerosols Loading Trends And Its Environmental Threats Over Cotonou-Benin, Nature Environment and Pollution Technology, 15 (3), 1111-1116
- [9] Emetere M.E., Akinyemi M. L., & Akinojo O., (2016): Effects Of Band Superposition On The Satellite Imagery Of Aerosol Optical Depth Over West Africa, Journal of Engineering and Applied Sciences 11(1), 17-22
- [10] Emetere M.E., Akinyemi M.L., & Akinojo O., (2015a): Parametric retrieval model for estimating aerosol size distribution via the AERONET, LAGOS station, Environmental Pollution, 207 (C), 381-390
- [11] Emetere M.E., Akinyemi M.L., & Akinojo O., (2015b): A Novel Technique for Estimating Aerosol Optical Thickness Trends Using Meteorological Parameters, 2015 PIAMSEE: AIP Conference Proceedings 1705, 020037 (2016); http://dx.doi.org/10.1063/1.4940285
- [12] Knapp, K. R., Frouin, R., Kondragunta, S., and Prados, A. (2005): Toward aerosol optical depth retrievals over land from GOES visible radiances: determining surface reflectance, Int. J. Remote Sens., 26, 4097–4116
- [13] MODIS, (2017): https://modis-atmos.gsfc.nasa.gov/MOD04_L2/format.html (Accessed 30th March, 2017).
- [14] Poschl, U. (2005): Atmospheric Aerosols: Composition, Transformation, Climate and Health Effects, Angew. Chem. Int. Edit., 44, 7520–7540
- [15] Levy, R. C., Remer, L. A., Mattoo, S., Vermote, E. F., and Kaufman, Y. J. (2007): Second-generation operational algorithm: retrieval of aerosol properties over land from inversion of Moderate Resolution Imaging Spectroradiometer spectral reflectance, J. Geophys. Res., 112, D13211
- [16] Lyapustin, A., Martonchik, J., Wang, Y., Laszlo, I., and Korkin, S. (2011): Multiangle implementation of atmospheric correction (MAIAC): Radiative transfer basis and lookup tables, J. Geophys. Res., 116, D03210
- [17] Vijayakumar, K. and Devara, P.C.S., (2013): Study of aerosol optical depth, ozone, and precipitable water vapour content over Sinhagad, a high-altitude station in the Western Ghats. International Journal of Remote Sensing, 34 (2): 613-630.

[18] Yang, Y., Liao, H. and Lou, S.-J., (2014): Simulated impacts of sulphate and nitrate aerosol formation on surface-layer ozone concentrations in China. Atmospheric and Oceanic Science Letters, 7(5): 441-446.